THE JOURNAL OF BIOLOGICAL CHEMISTRY VOL. 289, NO. 19, pp. 13112–13123, May 9, 2014

Tight Junctional Localization of Claudin-16 Is Regulated by Syntaxin 8 in Renal Tubular Epithelial Cells*[S]

Received for publication, December 6, 2013, and in revised form, March 18, 2014 Published, JBC Papers in Press, March 21, 2014, DOI 10.1074/jbc.M113.541193

Akira Ikari[‡§1], Chie Tonegawa[§], Ayumi Sanada[§], Toru Kimura[¶], Hideki Sakai[‖], Hisayoshi Hayashi[**], Hajime Hasegawa[‡‡], Masahiko Yamaguchi[§], Yasuhiro Yamazaki[§], Satoshi Endo[‡], Toshiyuki Matsunaga[‡], and Junko Sugatani[§]

From the [‡]Laboratory of Biochemistry, Department of Biopharmaceutical Sciences, Gifu Pharmaceutical University, Gifu 501-1196, Japan, the [§]School of Pharmaceutical Sciences, University of Shizuoka, Shizuoka 422-8526, Japan, the [¶]School of Medicine, Kyorin University, Tokyo, 181-8611, Japan, the [‖]Graduate School of Medicine and Pharmaceutical Sciences, University of Toyama, Toyama 930-0194, Japan, the [**]School of Food and Nutritional Sciences, University of Shizuoka, Shizuoka 422-8526, Japan, and the [‡‡]Saitama Medical Center, Saitama Medical University, Saitama 350-8550, Japan

Background: Disease-associated claudin-16 mutants cause mislocalization and decrease reabsorption of Mg^{2+} in the kidney.
Results: Knockdown of syntaxin 8 in kidney cells decreased the tight junctional localization of claudin-16 in parallel with a decrease in Mg^{2+} permeability.
Conclusion: Syntaxin 8 controls the localization of claudin-16.
Significance: Our findings provide a new insight into the trafficking mechanism of tight junctional proteins.

Claudin-16 (CLDN16) regulates the paracellular reabsorption of Mg^{2+} in the thick ascending limb of Henle's loop. However, the mechanism regulating the tight junctional localization of CLDN16 remains unknown. In yeast two-hybrid systems, we found that CLDN16 bound to syntaxin 8 (STX8), a target soluble *N*-ethylmaleimide-sensitive factor attachment protein receptor. We have examined the effect of STX8 on the localization and function of CLDN16 using Madin-Darby canine kidney cells expressing FLAG-tagged CLDN16. A pulldown assay showed that the carboxyl cytoplasmic region of human CLDN16 bound to STX8. CLDN16 was localized in the thick ascending limb, whereas STX8 was widely distributed throughout the rat kidney. An association between CLDN16 and STX8 was observed in rat renal homogenates and Madin-Darby canine kidney cells. STX8 siRNA decreased the cell surface localization of CLDN16 and transepithelial electrical resistance and permeability to Mg^{2+} but increased the co-localization of CLDN16 with early endosome and lysosome markers. Dephosphorylation of CLDN16 by protein kinase A inhibitors and S217A mutant, a dephosphorylated form, decreased the association with STX8 and the cell surface localization of CLDN16. Recycling assays indicated that STX8 siRNA decreased the trafficking of CLDN16 to the plasma membrane without affecting endocytosis. Dominant negative Rab11 and recycling inhibitor primaquine decreased the cell surface localization of CLDN16, which was similar to that in STX8 siRNA-transfected cells. These results suggest that STX8 mediates the recycling of CLDN16 and constitutes an important component of the CLDN16 trafficking machinery in the kidney.

The tight junction (TJ)[2] forms the most apical component of the lateral adhesion complex in epithelial cells and plays a central role in maintaining barrier and cell polarity. The TJ barrier contains aqueous channels capable of discriminating charge and molecular size, and its electrical resistance varies among different epithelia (1, 2). The TJ comprises a complex of multiple integral membrane, scaffolding, and signaling proteins. A number of integral membrane proteins associated with the TJ have been identified to date, including occludin (3) and claudins (CLDNs) (4–6). CLDNs are tetraspan proteins consisting of a family of >20 members in mammals. The cytoplasmic carboxyl-terminal PDZ binding motif in each claudin binds to scaffolding proteins such as ZO-1, ZO-2, and ZO-3. ZO-1 and ZO-2 indirectly link CLDNs to the actin cytoskeleton, and these junctional complexes are necessary to maintain the characteristics of permeability.

The kidney is composed of numerous nephrons, which have several segments. Each segment has a distinct expression pattern of CLDNs and role in the reabsorption of ions, water, and molecules. Most Mg^{2+} is reabsorbed via a paracellular pathway in the thick ascending limb (TAL) of Henle's loop (7). Familial hypomagnesemia with hypercalciuria and nephrocalcinosis (FHHNC) is characterized by progressive renal Mg^{2+} and Ca^{2+}

* This work was supported in part by Grant-in-Aid for Scientific Research (C) from the Japan Society for the Promotion of Science KAKENHI 23590263 and by grants from the Salt Science Research Foundation (1124), Takeda Science Foundation, and Research Foundation for Pharmaceutical Sciences (to A. I.).
[S] This article contains supplemental Table S1.
[1] To whom correspondence should be addressed: Laboratory of Biochemistry, Dept of Biopharmaceutical Sciences, Gifu Pharmaceutical University, 1-25-4 Daigaku-nishi, Gifu 501-1196, Japan. Tel.: 81-58-230-8124; Fax: 81-58-230-8124; E-mail: ikari@gifu-pu.ac.jp.

[2] The abbreviations used are: TJ, tight junction; MBP, maltose-binding protein; DN, dominant negative; CLDN, claudin; EEA1, early endosomal autoantigen 1; H-89, *N*-[2-(*p*-bromocinnamylamino)ethyl]-5-isoquinolinesulfonamide dihydrochloride; MDCK, Madin-Darby canine kidney; MESNA, sodium 2-mercaptoethanesulfonate; STX, syntaxin; TAL, thick ascending limb; TER, transepithelial electrical resistance; CLDN, claudin; FHHNC, familial hypomagnesemia with hypercalciuria and nephrocalcinosis; THP, Tamm-Horsfall glycoprotein; PKI, PKA inhibitor; ER, endoplasmic reticulum.

wasting, resulting in impaired renal function and renal failure. FHHNC has been genetically linked to mutations in the *CLDN16* or *CLDN19* gene (8, 9). CLDN16 and CLDN19 are both expressed in the TJ of the TAL of Henle's loop (10). A dysfunction in one or both of these may affect the reabsorption of Mg^{2+} in the TAL of Henle's loop, leading to hypomagnesemia. Various mutants of CLDN16 dissociate from the TJ and are distributed in the Golgi apparatus, endoplasmic reticulum, or lysosome. We previously reported that the dephosphorylated mutant of CLDN16 was distributed in the lysosome and showed little permeability to Mg^{2+} (11). CLDN16 mistargeting must cause hypomagnesemia, however, the regulatory mechanisms for trafficking of CLDN16 have not yet been clarified.

Membrane fusion is mostly mediated by the formation of specific complexes between cognate soluble *N*-ethylmaleimide-sensitive factor attachment protein receptor (SNARE) molecules on vesicles and target membranes. In combination with other regulatory factors including small GTPases (12) and early endosomal autoantigen 1 (EEA1) (13), SNAREs define the specificity of organellar fusion events (14). Among the SNARE family, syntaxins (STXs) belong to a subfamily of target-SNAREs stationed at the target membrane. The SNARE domain of STXs consists of a highly conserved coiled-coil domain and mediates the trafficking and targeting of intracellular vesicles. STXs also interact with a wide range of plasma membrane proteins and regulate their intracellular trafficking, including sodium channel (15), voltage-gated potassium channel (16), and cystic fibrosis transmembrane conductance regulator (17). However, it has not been known whether STXs regulate the intracellular trafficking of CLDNs.

In the present study we investigated the novel association protein of CLDN16, which can regulate its trafficking. In yeast two-hybrid systems we demonstrated that CLDN16 bound to STX8. Immunoprecipitation assays showed that CLDN16 bound to STX8 in the rat renal tubule. STX8 siRNA decreased the cell surface localization of CLDN16 and permeability to Mg^{2+} in Madin-Darby canine kidney (MDCK) cells expressing FLAG-tagged CLDN16. Furthermore, STX8 siRNA decreased the recycling of CLDN16 to the plasma membrane without affecting endocytosis. Our present results indicate that STX8 is involved in the trafficking of CLDN16 from intracellular compartments to the TJ.

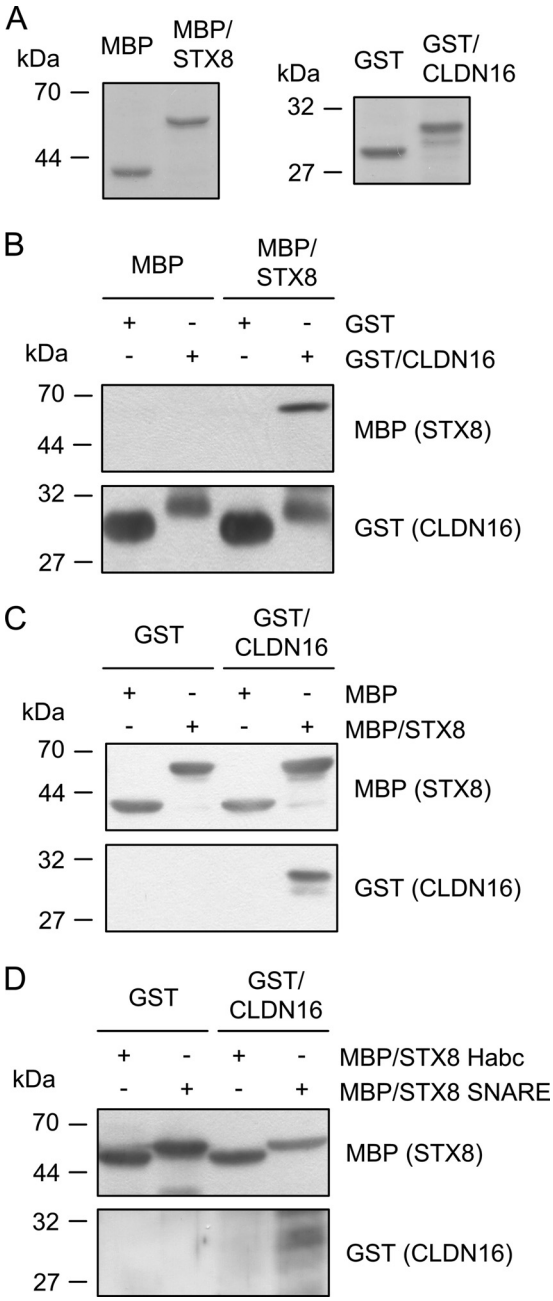

FIGURE 1. **Association of the carboxyl cytoplasmic region of CLDN16 with STX8.** *A*, the cytoplasmic region without the transmembrane domain of STX8 was fused with MBP (*MBP/STX8*). The carboxyl cytoplasmic region of CLDN16 was fused with GST (*GST/CLDN16*). Proteins were fractionated on gels and stained with Coomassie Brilliant Blue. *B*, GST and GST/CLDN16 bound to glutathione-Sepharose beads were incubated with MBP or MBP/STX8. Proteins on the beads were eluted with the sample buffer and immunoblotted with anti-MBP or GST antibody. *C*, MBP and MBP/STX8 bound to amylose-Sepharose beads were incubated with GST or GST/CLDN16. Proteins on the beads were immunoblotted with anti-MBP or GST antibody. *D*, the MBP protein was fused with the Habc domain (*MBP/STX8 Habc*) or SNARE motif (*MBP/STX8 SNARE*) of STX8. Proteins bound to amylose-Sepharose beads were incubated with GST or GST/CLDN16. Proteins on the beads were immunoblotted with anti-MBP or GST antibody.

EXPERIMENTAL PROCEDURES

Materials—Rabbit anti-CLDN1, CLDN16, and ZO-1 antibodies were obtained from Zymed Laboratories Inc. (South San Francisco, CA). Rabbit anti-FLAG and mouse anti-myc antibodies were from Medical & Biological Laboratories Co. (Nagoya, Japan). The mouse anti-FLAG antibody and sodium 2-mercaptoethanesulfonate (MESNA) were from Wako Pure Chemical Industries (Osaka, Japan). Mouse anti-BiP, EEA1, GM130, and STX8 antibodies and doxycycline were from BD Biosciences Clontech (Mountain View, CA). The rabbit anti-LIMPII antibody was from Novus (Littleton, CO). The rabbit anti-Tamm-Horsfall glycoprotein (THP) antibody was from Santa Cruz. The goat anti-glutathione *S*-transferase (GST) antibody was from GE Healthcare. Mouse anti-maltose-binding protein (MBP) was from New England Biolabs (Ipswich, MA). Mouse anti-phosphoserine (p-Ser) was from Sigma. *N*-[2-(*p*-Bromocinnamylamino)ethyl]-5-isoquinolinesulfonamide (H-89) was from LKT Laboratories (St. Paul, MN). Myristoy-

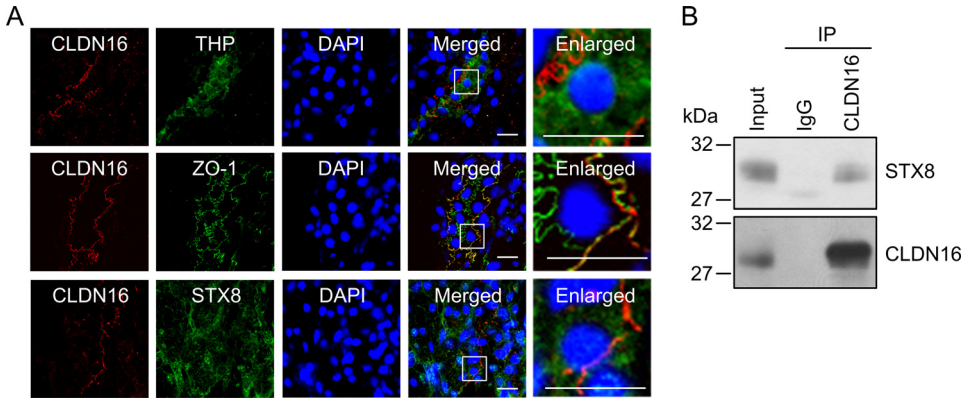

FIGURE 2. **Association between CLDN16 and STX8 in the rat kidney.** *A*, tissue sections were stained with anti-CLDN16 (*red*) plus THP, STX8, or ZO-1 (*green*) antibodies in the presence of DAPI (*blue*). The *right panels* show enlarged images. The *scale bars* represent 10 μm. *B*, immunoprecipitation (*IP*) using control rabbit IgG or anti-CLDN16 antibody was performed in the homogenates of the renal cortex. The detergent extracts (*Input*) and immune pellets were immunoblotted with anti-STX8 or CLDN16 antibody.

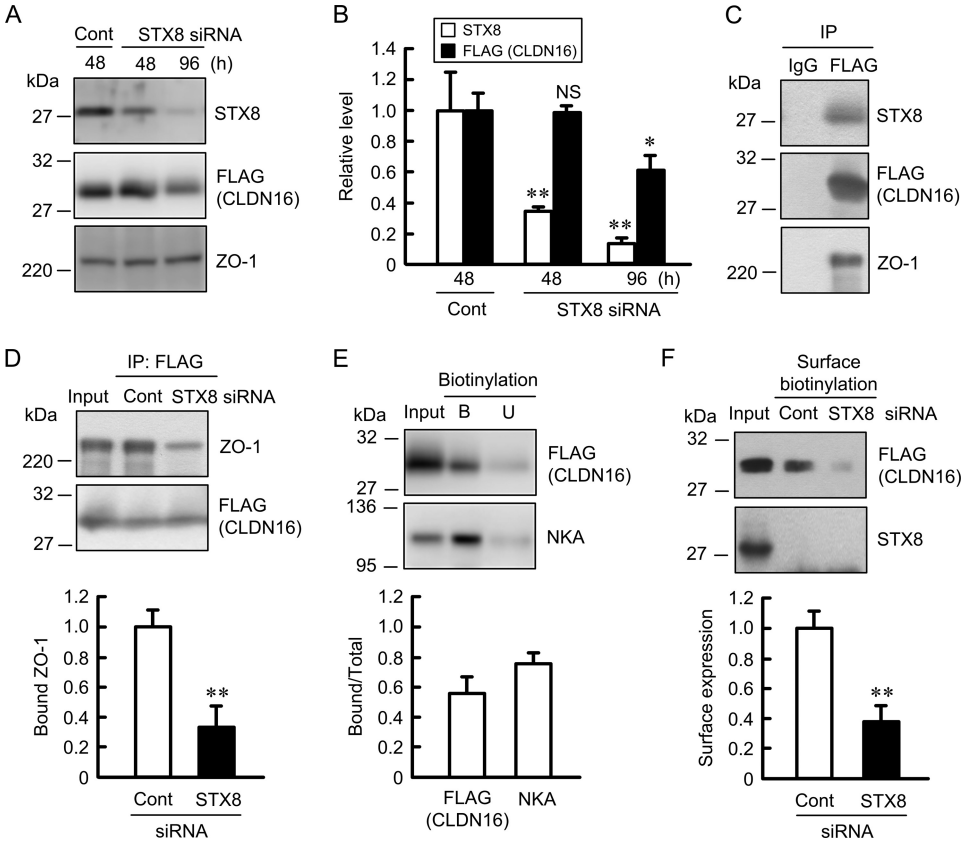

FIGURE 3. **Decrease in the cell surface localization of CLDN16 by STX8 siRNA.** *A*, cells were transfected with negative control or STX8 siRNA. Cell lysates were collected after 48 and 96 h of transfection and immunoblotted with anti-STX8, FLAG, and ZO-1 antibodies. *B*, expression levels of STX8, FLAG, and ZO-1 in the STX8 siRNA-transfected cells were compared with those in the control siRNA-transfected cells. *C*, the lysates from control cells were immunoprecipitated (*IP*) with mouse IgG or anti-FLAG antibody. Immune pellets were immunoblotted with anti-STX8, FLAG, or ZO-1 antibody. *D*, the lysates from control and STX8-siRNA-transfected cells were immunoprecipitated with anti-FLAG antibody. The detergent extracts (*Input*) and immune pellets were immunoblotted with anti-ZO-1 or FLAG antibody. The bound ZO-1 was expressed relative to the value in cells transfected with control siRNA. *E*, the detergent extracts (*Input*), bound pellets (*B*), and unbound supernatants (*U*) were immunoblotted with anti-FLAG or Na^+/K^+-ATPase α subunit (*NKA*) antibody. The bound amount of FLAG-tagged CLDN16 and NKA was expressed relative to the total amount (bound + unbound). *F*, the detergent extracts (*Input*) and cell surface-biotinylated proteins were immunoblotted with anti-FLAG or STX8 antibody. The cell surface localization of FLAG-tagged CLDN16 was expressed relative to the value in cells transfected with control siRNA. $n = 3–4$. **, $p < 0.01$ significantly different from the control. *NS*, not significantly different.

lated PKA inhibitor 14-22 amide (PKI) was from Merck Millipore (Billerica, MA). Lipofectamine 2000 was from Invitrogen. All other reagents were of the highest grade of purity available.

Yeast Two-hybrid Screening—The interacting protein of CLDN16 was screened using the Matchmaker Gold Yeast Two-hybrid System (Clontech). The carboxyl cytoplasmic region of human CLDN16 was amplified by PCR using a set of sense (5′-GAATTCAAAGATGTTGGACCTGAGAG-3′) and antisense (5′-GGATCCTTACACCCTTGTGTCTAC-3′) primers containing custom EcoRI and BamHI restriction sites, respectively. The PCR product was cloned into the pGBKT7 bait vector. The vector was introduced into the Y2HGold strain fol-

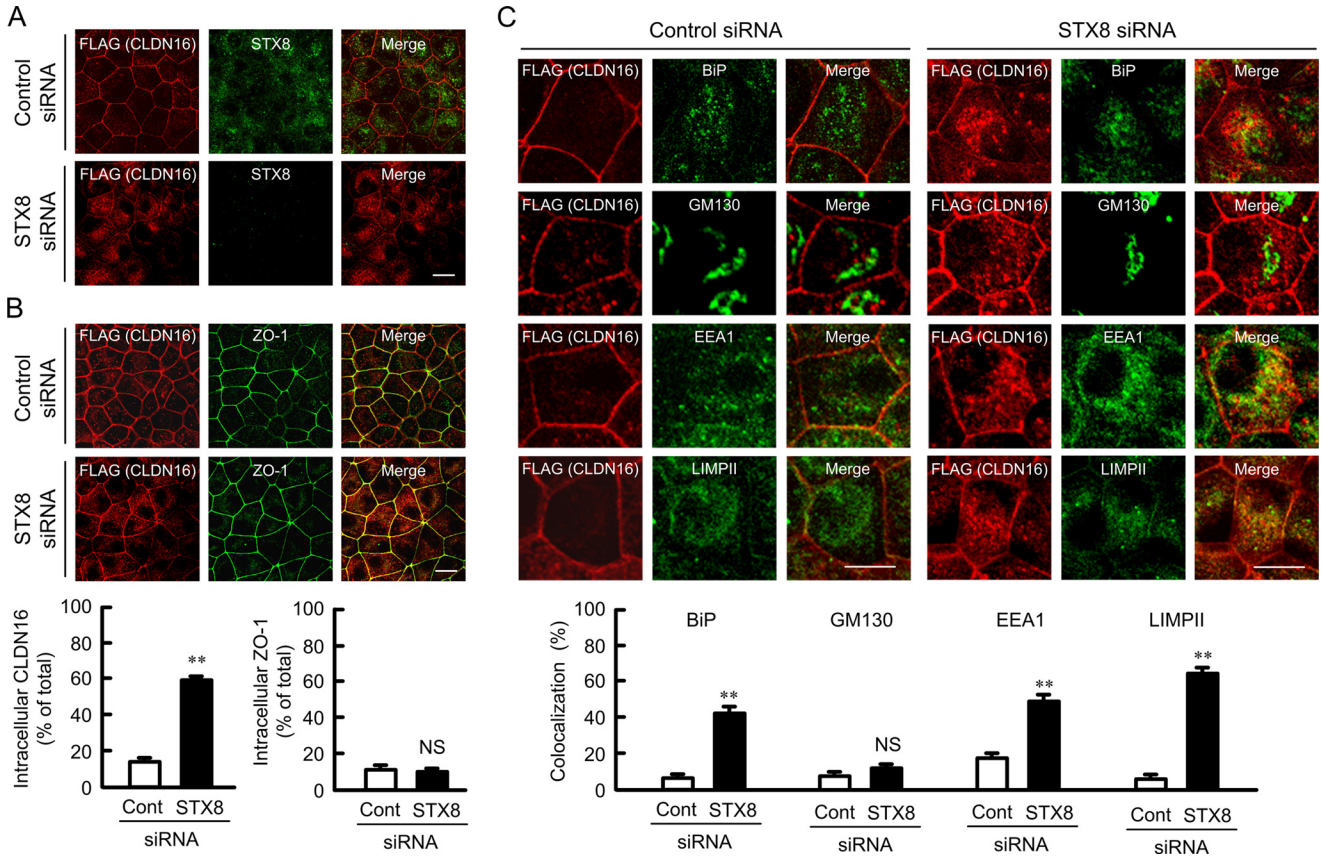

FIGURE 4. **Effect of STX8 siRNA on subcellular localization of CLDN16.** *A*, cells transfected with negative control or STX8 siRNA were stained with anti-FLAG (*CLDN16*) and STX8 antibodies. *B*, cells transfected with negative control or STX8 siRNA were stained with anti-FLAG (CLDN16) and ZO-1 antibodies (*upper images*). The fluorescence intensities of intracellular CLDN16 (*lower left*) or ZO-1 (*lower right*) were shown as the percentage of those of total (intracellular and tight junctional) CLDN16 or ZO-1 ($n = 55–69$ cells from over five separates experiments). *C*, cells transfected with negative control or STX8 siRNA were stained with anti-FLAG (*CLDN16*) plus BiP (ER marker), GM130 (Golgi marker), EEA1 (early endosome marker), or LIMPII (lysosome marker) antibodies (*upper images*). The co-localization of intracellular CLDN16 with organelle markers was shown as the percentage ($n = 53–102$ cells from over five separates experiments). The *scale bars* represent 5 μm. **, $p < 0.01$; *NS*, not significantly different from the control.

lowed by selection on medium lacking tryptophan. The pGADT7 vector transformed with a human kidney cDNA library was introduced into the Y187 strain. After combining the library strain with the bait strain, yeast transformants were plated on synthetic complete medium lacking adenine, histidine, leucine, and tryptophan. Ninety-four positive clones were picked up, and the sequences of these inserts were determined. Sequencing was performed by Bio Matrix Research (Chiba, Japan).

Pulldown Assay—The carboxyl cytoplasmic region of human CLDN16 was subcloned into the pGEX4T1 vector (GE Healthcare). The cytoplasmic region of STX8 without the transmembrane domain was amplified by PCR using a set of sense (5′-GATATCATGACTGGGTTGTCGATGG-3′) and antisense (5′-GAATTCTTACGGCTCATCTTCATTG-3′) primers containing custom EcoRV and EcoRI restriction sites, respectively. The PCR product was cloned into the pMAL-c5x vector (New England Biolabs). These vectors were introduced into *Escherichia coli* BL21 and grown in the overnight express. GST-fused and MBP-fused proteins were purified with glutathione-Sepharose 4B and amylose resin beads, respectively. The beads were incubated in a buffer composed of 10 mM Tris-HCl (pH 7.5), 150 mM NaCl, 0.1% Nonidet P-40, 2 mM EDTA, 1 mM phenylmethylsulfonyl fluoride, and protease inhibitor mixture for 12 h at 4 °C. Bound proteins were then eluted with a sample buffer and applied to the SDS-polyacrylamide gel. Proteins were blotted onto a PVDF membrane and incubated with each primary antibody followed by a peroxidase-conjugated secondary antibody. The blots were visualized as described in the immunoblotting section.

Cell Culture and Transfection—The MDCK Tet-OFF cell line was obtained from BD Biosciences Clontech. Cells expressing FLAG-tagged wild type and S217A mutant CLDN16 were generated in our laboratory (18). Cells were grown in Dulbecco's modified Eagle's medium (Sigma) supplemented with 5% fetal calf serum (HyClone, Logan, UT), 0.07 mg/ml penicillin-G potassium, 0.14 mg/ml streptomycin sulfate, 0.1 mg/ml G418, and 0.1 mg/ml hygromycin B in a 5% CO_2 atmosphere at 37 °C. Wild type Rab11 (pSRa-neo-myc-Rab11) and dominant negative Rab11 (N25Rab11) vectors were kindly gifted from Prof. Y. Takai (Kobe University, Japan). The Rab11 vectors, STX8 siRNA, and negative control siRNA (Santa Cruz Biotechnology) were transfected into cells using Lipofectamine 2000 as recommended by the manufacturer.

Preparation of Renal Homogenates, Cell Lysates, and Immunoprecipitation—Male Wistar rats (170–230 g, Nippon SLC, Shizuoka, Japan) were fed standard laboratory chow and allowed free access to drinking water. Rats were humanely

killed in accordance with the guidelines presented by the Institute Animal Care and Life Committee of University of Shizuoka, and their kidneys were isolated. The homogenates of the renal cortex were prepared as described previously (19). Confluent MDCK cells were scraped into cold PBS and precipitated by centrifugation. The cells were then lysed in a radioimmune precipitation assay buffer containing 150 mM NaCl, 0.5 mM EDTA, 1% Triton X-100, 50 mM Tris-HCl (pH 8.0), protease inhibitor mixture (Sigma), and 1 mM phenylmethylsulfonyl fluoride and were then sonicated for 20 s. After centrifugation at 1000 × *g* for 5 min, the supernatant was collected (cell lysates). In an immunoprecipitation assay, renal homogenates and cell lysates were incubated with protein G-Sepharose and anti-FLAG antibody or anti-CLDN16 antibody at 4 °C for 16 h with gentle rocking. After centrifugation at 6000 × *g* for 1 min, the pellet was washed 3 times with the radioimmune precipitation assay buffer. In a biotinylation assay, cell surface proteins were biotinylated as described previously (20). The cell lysates, immunoprecipitates, and biotinylated proteins were solubilized in a sample buffer for SDS-polyacrylamide gel electrophoresis. To estimate efficiency of biotinylation and streptavidin precipitation, we analyzed the level of Na^+/K^+-ATPase α subunit, which is predominantly localized in the plasma membrane. In addition, the extent of protein adsorption onto streptavidin-agarose beads was assessed. Protein concentrations were measured by a protein assay kit (Bio-Rad) in which bovine serum albumin was used as a standard.

SDS-Polyacrylamide Gel Electrophoresis and Immunoblotting—SDS-polyacrylamide gel electrophoresis was performed as described previously (21). Briefly, cell lysates or immunoprecipitates were applied to the SDS-polyacrylamide gel. Proteins were blotted onto a PVDF membrane and incubated with each primary antibody followed by a peroxidase-conjugated secondary antibody. Finally, the blots were stained with an ECL Western blotting kit (GE Healthcare).

Measurement of Transepithelial Electrical Resistance (TER) and Paracellular Permeability—MDCK cells expressing FLAG-tagged CLDN16 were plated at confluent densities on transwells with polyester membrane inserts (Corning Inc.-Life Sciences, Acton, MA). TER and paracellular permeability to FITC-dextran and Mg^{2+} were measured as described previously (22).

Confocal Microscopy—Rat kidney slices and MDCK cells expressing FLAG-tagged CLDN16 were immunostained as described previously (23). Immunolabeled cells were visualized on an LSM 510 confocal microscope (Carl Zeiss) set with a filter appropriate for Alexa Fluor 488 (488-nm excitation, 530-nm emission) and Alexa Fluor 546 (543-nm excitation, 585–615-nm emission). Fluorescence intensities of CLDN16 and ZO-1 were determined by measuring the mean pixel density of staining area using ImageJ software (National Institute of Health, Bethesda, MD). The image area containing the signal from the TJ (ZO-1 signal) was manually marked using ImageJ. The area below the ZO-1 area was defined as the cell interior. After subtraction of background, the intracellular intensities of CLDN16 or ZO-1 were shown as percentage of total (intracellular and tight junctional) intensities of CLDN16 or ZO-1.

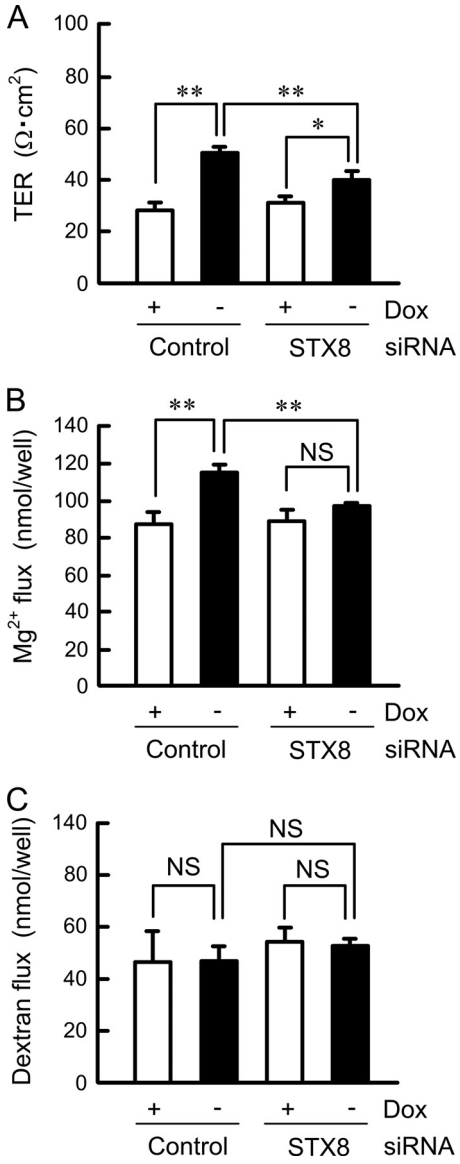

FIGURE 5. **Effect of STX8 siRNA on paracellular permeability.** Cells transfected with negative control or STX8 siRNA were cultured on transwell inserts for 3 days in the presence and absence of 100 ng/ml doxycycline (*Dox*). FLAG-tagged CLDN16 was expressed in the absence of doxycycline. *A*, TER was measured with a volt ohmmeter. *B*, transepithelial Mg^{2+} permeability from the apical to basal compartment was measured using XB-1. *C*, FITC-dextran permeability from the apical to basal compartments was measured. FITC-dextran (4000 Da, 0.5 mg/ml) was applied to the apical compartment. The buffer in the basal compartment was collected after 1 h, and fluorescence intensity was measured. $n = 4$. **, $p < 0.01$; *NS*, not significantly different.

Statistics—Results are presented as the mean ± S.E. Differences between groups were assessed with a one-way analysis of variance, and corrections for multiple comparisons were made using Tukey's multiple comparison test. Significant differences were assumed at $p < 0.05$.

RESULTS

Association of CLDN16 with STX8 in the Pulldown Assay—To identify novel CLDN16-binding proteins involved in the regulation of its trafficking, we performed yeast two-hybrid screening using a human kidney cDNA library with the carboxyl cytoplasmic region of CLDN16 as bait. We obtained 234

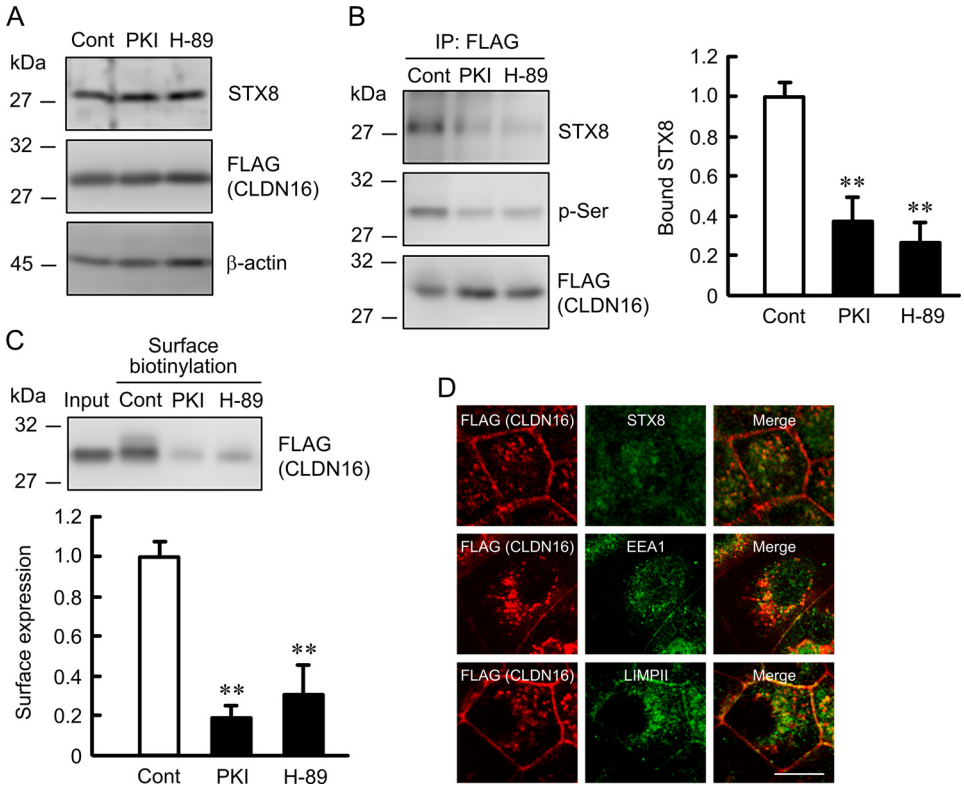

FIGURE 6. **Decrease in the cell surface localization of CLDN16 by PKA inhibitors.** Cells expressing FLAG-tagged CLDN16 were incubated with 10 μM PKI or 50 μM H-89 for 1 h. *A*, cell lysates were immunoblotted with anti-STX8, FLAG, and β-actin antibodies. *B*, the lysates from control and PKA inhibitors-treated cells were immunoprecipitated (*IP*) with anti-FLAG antibody, and the immune pellets were immunoblotted with anti-STX8, p-Ser, or FLAG antibody. The bound STX8 was expressed relative to the value in control cells. *C*, the detergent extracts (*Input*) and cell surface-biotinylated proteins were immunoblotted with anti-FLAG antibody. The cell surface localization of FLAG-tagged CLDN16 was expressed relative to the value in control cells. *D*, the cells incubated with PKI were stained with anti-FLAG (CLDN16) plus STX8, EEA1, or LIMPII antibodies. The *scale bar* represents 5 μm. $n = 3$. **, $p < 0.01$ significantly different from the control.

positive clones, the sequences of which were determined. A homology search of the GenBank™ and EMBL sequence databases was performed using the program FASTA. Interactors of CLDN16 identified in yeast two-hybrid screening were shown in supplemental Table S1. Multiple-PDZ domain protein-1 (13 clones) and membrane-associated guanylate kinase (3 clones) were identified, and these proteins have been reported to be localized in the TJ (24–26). We chose STX8 (25 clones) as a candidate protein involved in regulating the trafficking of CLDN16 because no candidate proteins other than STX8 were found. To examine the association between CLDN16 and STX8, we made a GST fusion protein to the carboxyl cytoplasmic region of CLDN16 and MBP fusion protein to the cytoplasmic region of STX8 (Fig. 1*A*). In the pulldown assay, CLDN16 was associated with the cytoplasmic region of STX8 (Fig. 1, *B* and *C*). STX8 has conserved helical domains (Habc) and a SNARE domain. The MBP protein containing a SNARE domain potentially bound to CLDN16, whereas the Habc domain was weak (Fig. 1*D*). These results indicate that the carboxyl cytoplasmic region of CLDN16 is associated with the SNARE domain of STX8.

Expression and Distribution of STX8 and CLDN16 in the Rat Kidney—CLDN16 was previously shown to be exclusively expressed in the TAL of Henle's loop in humans (8), mice (27), and bovines (28). In the rat kidney CLDN16 was localized in the cells expressing THP, a marker of the TAL, in the rat kidney (Fig. 2*A*). The subcellular localization pattern of CLDN16 was merged with ZO-1, a marker of the TJ. STX8 was widely expressed in the renal tubules including CLDN16-positive cells. STX8 was immunoprecipitated by anti-CLDN16 antibody but not by mouse IgG (Fig. 2*B*). These results indicate that CLDN16 may be associated with STX8 in the kidney.

Decrease in Cell Surface Localization of CLDN16 by STX8 siRNA—The introduction of STX8 siRNA into MDCK cells decreased STX8 expression without affecting ZO-1 expression in the cells (Fig. 3, *A* and *B*). The expression of CLDN16 was unchanged after 48 h and significantly decreased after 96 h of the introduction of STX8 siRNA. CLDN16 was co-immunoprecipitated with STX8 and ZO-1 (Fig. 3*C*). Müller *et al.* (29) reported that the association of CLDN16 with ZO-1 is necessary for the tight junctional localization of CLDN16. We found that STX8 siRNA weakened the association between CLDN16 and ZO-1 (Fig. 3*D*), suggesting that STX8 siRNA decreases cell surface localization of CLDN16. We performed the cell surface biotinylation assay to quantify the level of CLDN16 at the plasma membrane. This approach has been used to examine the cell surface localization of CLDN1, CLDN2, and CLDN4 in MDCK cells (20, 30, 31). To estimate the efficiency of biotinylation and streptavidin precipitation, we also analyzed the level of Na^+/K^+-ATPase α subunit, which is predominantly localized in the plasma membrane. The bound/total ratio of CLDN16 was similar to that of Na^+/K^+-ATPase α subunit (Fig.

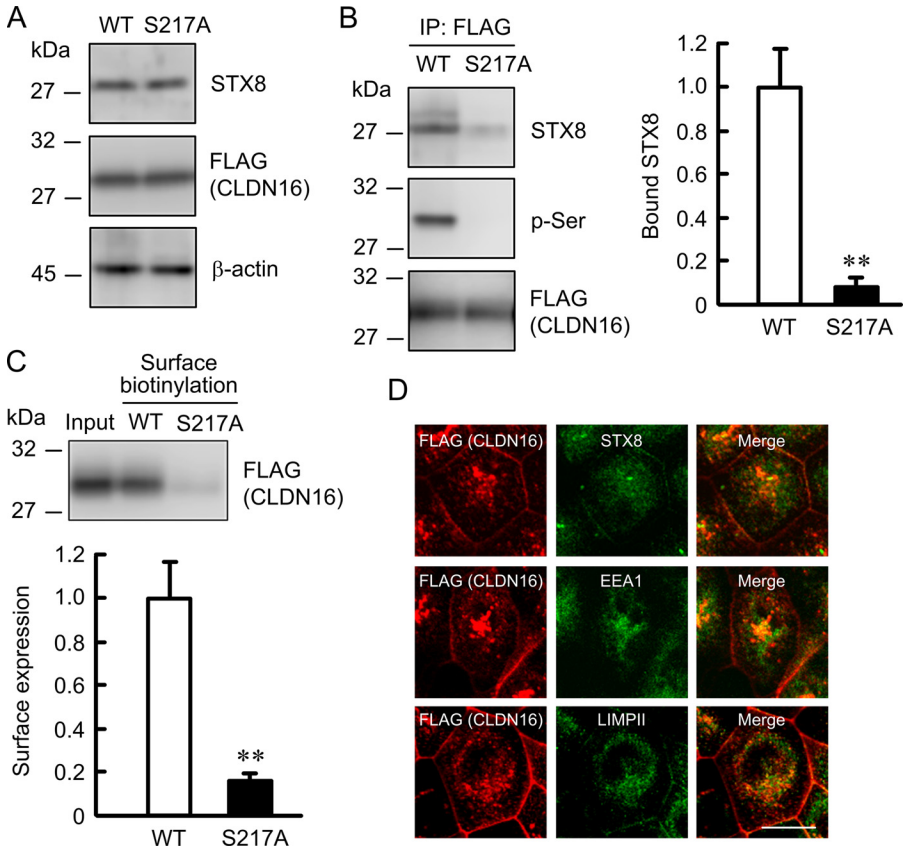

FIGURE 7. **Co-localization of S217A mutant CLDN16 with STX8.** FLAG-tagged WT or S217A mutant CLDN16 was expressed in MDCK cells. *A*, cell lysates were immunoblotted with anti-STX8, FLAG, and β-actin antibodies. *B*, the lysates were immunoprecipitated (*IP*) with anti-FLAG antibody, and immune pellets were immunoblotted with anti-STX8, p-Ser, or FLAG antibody. The bound STX8 was expressed relative to the value in control cells. *C*, the detergent extract of WT (*Input*) and cell surface-biotinylated proteins were immunoblotted with anti-FLAG antibody. The cell surface localization of FLAG-tagged CLDN16 was expressed relative to the value in WT. *D*, cells expressing S217A mutant of FLAG-tagged CLDN16 were stained with anti-FLAG (*CLDN16*) plus STX8, EEA1, or LIMPII antibodies. The *scale bar* represents 5 μm. $n = 3$. **, $p < 0.01$ significantly different from WT.

3*E*), suggesting that the cell surface CLDN16 was fully biotinylated in the present experiments. The level of cell surface localization of CLDN16 in the STX8 siRNA-transfected cells was significantly lower than that in the control siRNA-transfected cells (Fig. 3*F*). The intracellular localization of CLDN16 and STX8 was examined using immunofluorescence. STX8 was mainly distributed in the cytoplasmic compartments. The green signal of STX8 disappeared by transfection of STX8 siRNA (Fig. 4*A*). CLDN16 was distributed in the cell-cell border area concomitant with ZO-1 in cells transfected with control siRNA (Fig. 4*B*). STX8 siRNA significantly increased the intracellular red signal of CLDN16 without affecting the green signal of ZO-1. We stained cells with BiP, an endoplasmic reticulum (ER) marker, GM130, a Golgi marker, EEA1, an early endosome marker, and LIMPII, a lysosome marker, to examine the subcellular localization of CLDN16. CLDN16 was co-localized with BiP, EEA1, and LIMPII but not with GM130 in STX8 siRNA-transfected cells (Fig. 4*C*). These results suggest that STX8 is involved in the intracellular trafficking from ER to Golgi apparatus and from early endosome to plasma membrane.

Effect of STX8 siRNA on Paracellular Permeability—In the MDCK cells, induction of CLDN16 expression by removing doxycycline caused an increase in TER and paracellular Mg^{2+} flux without affecting dextran flux (Fig. 5). STX8 siRNA significantly inhibited the CLDN16-induced increase in TER and Mg^{2+} flux. These results indicate that CLDN16 is functionally expressed in the cells, and STX8 siRNA inhibits the function of CLDN16.

Effects of PKA Inhibitors on the Intracellular Localization of CLDN16—We previously reported that the tight junctional localization of CLDN16 was regulated by PKA (11). PKI and H-89, PKA inhibitors, did not change the expression of STX8 or CLDN16 but decreased the phosphoserine level of CLDN16 and association between CLDN16 and STX8 (Fig. 6, *A* and *B*). Furthermore, PKI and H-89 significantly decreased the cell surface localization of CLDN16 (Fig. 6*C*). Despite the dissociation of CLDN16 from STX8 by PKI, CLDN16 was co-localized with STX8, EEA1, and LIMPII (Fig. 6*D*). Similarly, S217A mutant CLDN16, a dephosphorylated form, was not associated with STX8 and was co-localized with STX8, EEA1, and LIMPII (Fig. 7). These results suggest that dephosphorylated CLDN16 can be distributed in the early endosome and lysosome concomitant with STX8 without their direct association. The phosphorylation of CLDN16 is necessary for the association with STX8 and the localization at the TJ.

Decrease in the Cell Surface Localization of CLDNs by Low Temperature—We examined the effect of low temperature on the subcellular localization of CLDN16. Cells were cooled to 20 °C and incubated for 1 h to block the transport of protein

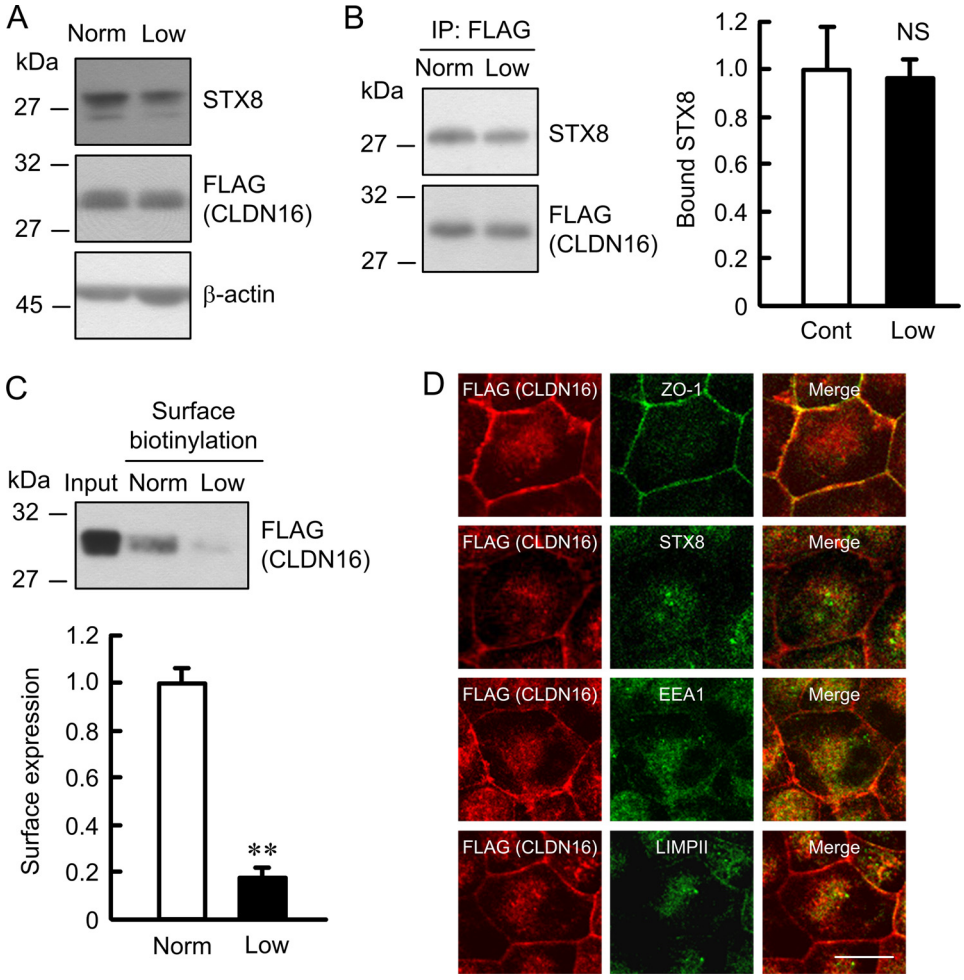

FIGURE 8. **Decrease in the cell surface localization of CLDN16 by a low temperature.** *A*, cells were incubated at normal (37 °C) or low temperature (20 °C) for 1 h. Cell lysates were immunoblotted with anti-STX8, FLAG, and β-actin antibodies. *B*, the lysates from normal and low temperature-treated cells were immunoprecipitated (*IP*) with anti-FLAG antibody. Immune pellets were immunoblotted with anti-STX8 or FLAG antibody. The bound STX8 was expressed relative to the value in normal cells. *C*, the detergent extracts (*Input*) and cell surface-biotinylated proteins were immunoblotted with anti-FLAG antibody. The cell surface localization of FLAG-tagged CLDN16 was expressed relative to the value in normal cells. *D*, cells treated with low temperature for 1 h were stained with anti-FLAG (CLDN16) plus ZO-1, STX8, EEA1, or LIMPII antibodies. The *scale bar* represents 5 μm. $n = 3–4$. **, $p < 0.01$; *NS*, not significantly different from the control.

from the endosomes to the plasma membrane. Low temperatures had no effects on the total expression level of STX8 and CLDN16 or the association between STX8 and CLDN16 (Fig. 8, *A* and *B*). The cell surface localization of CLDN16 was lower at 20 °C than at the control temperature (Fig. 8*C*). Similar to Western blotting, the low temperature increased the intracellular red signal of CLDN16 and induced the co-localization of CLDN16 with STX8, EEA1, and LIMPII (Fig. 8*D*). These results suggest that low temperature can inhibit the trafficking pathway of CLDN16.

Effect of STX8 siRNA on Endocytosis and Exocytosis of CLDN16—The inhibition of the association between CLDN16 and STX8 may decrease the trafficking of CLDN16 from subcellular compartments to the TJ or increase its trafficking from the TJ to subcellular compartments. Therefore, we examined the effect of STX8 siRNA on the endocytosis and exocytosis of CLDN16. In the endocytosis assay the internalization of CLDN16 was the same in both control and STX8 siRNA-transfected cells (Fig. 9*A*). In contrast, the externalization of CLDN16 in the STX8 siRNA-transfected cells was slower than that in the control siRNA-transfected cells (Fig. 9*B*). These results suggest that STX8 is involved in the exocytosis of CLDN16 from subcellular compartments to the TJ.

Decrease in Cell Surface Localization of CLDN16 by DN-Rab11 and Primaquine—The trafficking of some plasma membrane proteins from recycling endosomes to the plasma membrane is regulated by Rab11 (32–34). We examined the effect of DN-Rab11 on the cell surface localization of CLDN16 in MDCK cells. The expression of WT- and DN-Rab11 was assessed using anti-myc-tag antibody (Fig. 10*A*). Neither WT- nor DN-Rab11 affected the expression of CLDN16 or STX8 in the cells. The cell surface localization of CLDN16 in the DN-Rab11-transfected cells was significantly lower than that in the WT-Rab11-transfected cells (Fig. 10*B*). Consistent with the results in Fig. 10*B*, DN-Rab11 increased the intracellular red signal of CLDN16 and induced the co-localization of CLDN16 with STX8, EEA1, and LIMPII (Fig. 10*C*). We then examined the effect of primaquine, a recycling inhibitor, on the cell surface localization of CLDN16. Similar to DN-Rab11, primaquine decreased the cell surface local-

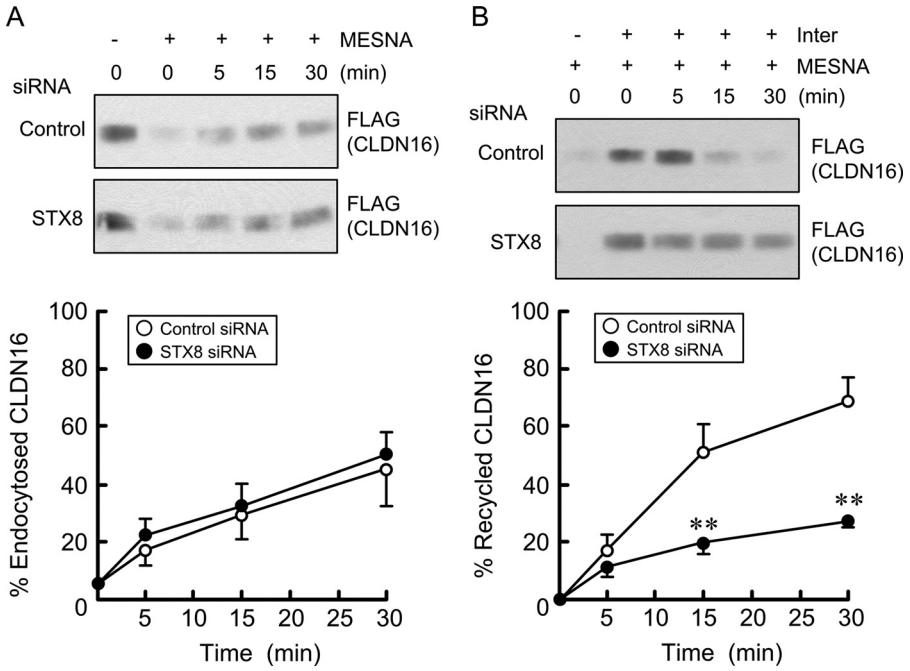

FIGURE 9. **Effect of STX8 siRNA on endocytosis and exocytosis of CLDN16.** Cells expressing FLAG-tagged CLDN16 were transfected with negative control or STX8 siRNA. *A*, plasma membrane proteins were biotinylated and then incubated for 5, 15, and 30 min at 37 °C. Proteins remaining at the cell surface were stripped of biotin with MESNA. Internalized CLDN16 was collected and immunoblotted with anti-FLAG antibody. The band density of FLAG was expressed relative to the value in the absence of MESNA. *B*, plasma membrane proteins were biotinylated and then internalized for 60 min at 37 °C. Proteins remaining at the cell surface were stripped of biotin with MESNA. Internalized CLDN16 (biotinylated) was incubated for 5, 15, and 30 min at 37 °C and recycled to the plasma membrane. Proteins expressing at the cell surface were then stripped of biotin with MESNA again. Non-recycled CLDN16 was collected and immunoblotted with anti-FLAG antibody. Recycling of CLDN16 was calculated from the band density of FLAG remaining in the cells after 5, 15, and 30 min relative to the value at 0 min. $n = 4$. **, $p < 0.01$ significantly different from the control.

ization of CLDN16 and increased the intracellular distribution of CLDN16 (Fig. 11). These results suggest that the cell surface localization of CLDN16 is regulated by a Rab11-dependent recycling pathway.

DISCUSSION

FHHNC has been genetically linked to mutations in the *CLDN16* or *CLDN19* gene (8, 9). A dysfunction in one or both of them may affect the reabsorption of Mg^{2+} in the TAL of Henle's loop, leading to hypomagnesemia. More than 40 mutations have been currently identified in *CLDN16* genes, whereas only 3 mutations have been identified in *CLDN19* genes (35). Mutations in *CLDN16* genes affect 28 different amino acids, which mainly occur in the extracellular loop and transmembrane domain. The mutants distributed in the TJ have full or partial function after being transfected into LLC-PK_1 (36) and MDCK-C7 cells (37). In contrast, the mutants mislocalized to the cytoplasmic compartments including the endoplasmic reticulum, Golgi apparatus, and lysosome lose their function. None of the mutations was shown to affect either of the two extracellular loops that had been considered to play an important role in conveying divalent cation permeability to the TJ (8). Therefore, the subcellular trafficking step of CLDN16 from intracellular compartments to the TJ plays an important role in controlling Mg^{2+} reabsorption.

The non-genomic regulation of the tight junctional localization of CLDN16 has not been examined in detail. Our recent studies revealed that the phosphorylation of CDLN16 by PKA was necessary for its localization at the TJ and that dephosphorylated CLDN16 was translocated to the lysosome (11). The CLDN16 phosphorylation may play an important role under physiological and pathophysiological conditions. Blood pressure is inversely associated with body Mg^{2+} levels (39), and dietary Mg^{2+} supplementation suppresses the development of hypertension (40). The phosphoserine level of CLDN16 has been shown to decrease in Dahl salt-sensitive hypertensive rats, which suggests that Mg^{2+} reabsorption was mediated via CLDN16 to be reduced in hypertensive rats (19). Furthermore, the phosphoserine level of CLDN16 was reported to be reduced by high concentrations of extracellular divalent cations in the blood side, suggesting that the dissociation of CLDN16 from the TJ at high Mg^{2+} concentrations prevents the excess reabsorption and backflow of Mg^{2+} from the peritubular space to the tubule lumen (41).

Even though the mislocalization of CLDN16 causes it to lose its function, its trafficking mechanism has not been clarified in detail. We have showed that STX8 was involved in the trafficking of CLDN16. STX8 has been reported to be ubiquitously expressed in invertebrate tissues including the kidney and distributed mainly in the ER, early endosome, late endosome, and lysosome (42). Immunofluorescence revealed that STX8 was mainly distributed in cytoplasmic compartments in the rat kidney and MDCK cells (Figs. 2 and 4). In contrast, CLDN16 was localized in the TJ concomitant with ZO-1. STX8 siRNA increased the cytoplasmic distribution of CLDN16, especially in the ER, early endosome, and lysosome (Fig. 4), suggesting that STX8 has an effect on these organelles. In the cell surface

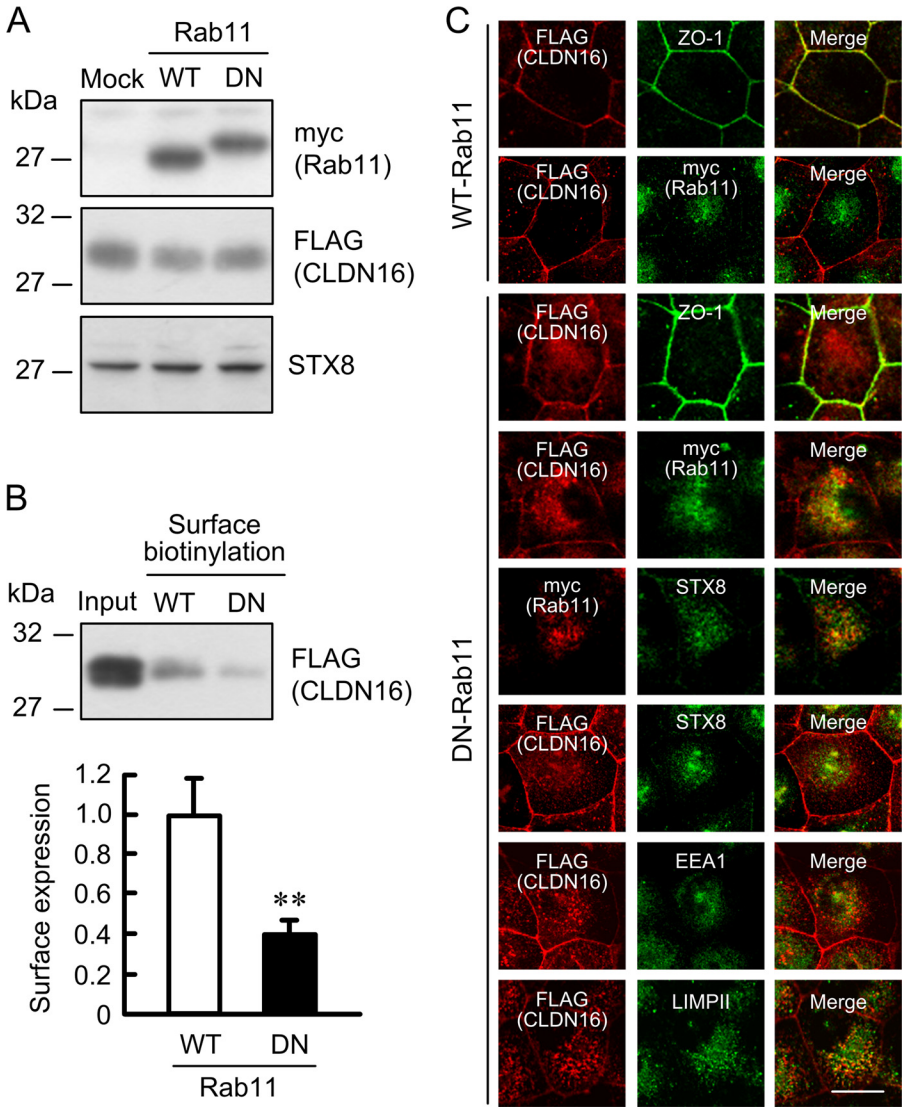

FIGURE 10. **Decrease in the cell surface localization of CLDN16 by DN-Rab11.** Cells expressing FLAG-tagged CLDN16 were transfected with the mock, WT-, or DN-Rab11 vector. *A*, cell lysates were immunoblotted with anti-myc, FLAG, and STX8 antibodies. *B*, the detergent extracts (*Input*) and cell surface-biotinylated proteins were immunoblotted with anti-FLAG antibody. The cell surface localization of FLAG-tagged CLDN16 was expressed relative to the value in cells transfected with WT-Rab11. *C*, cells transfected with the WT- or DN-Rab11 vector were stained with anti-FLAG (CLDN16), ZO-1, myc (Rab11), STX8, EEA1, and LIMPII antibodies. The *scale bar* represents 5 μm. $n = 4$. **, $p < 0.01$ significantly different from WT.

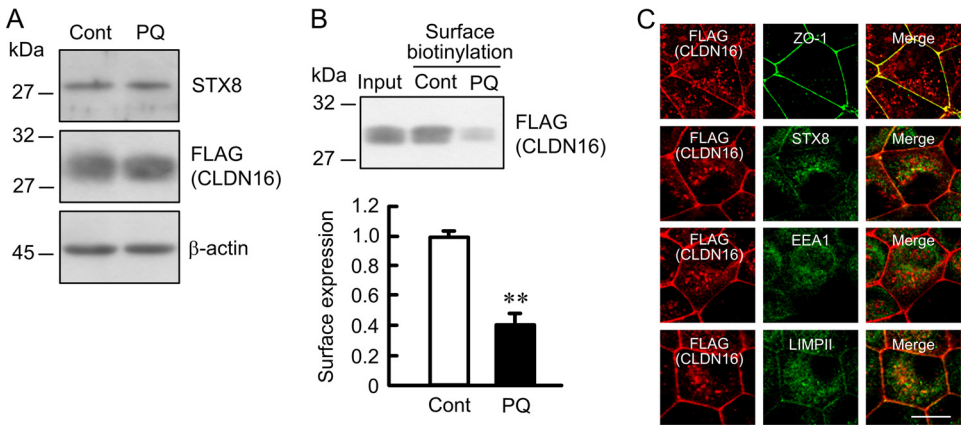

FIGURE 11. **Decrease in cell surface localization of CLDN16 by primaquine.** Cells expressing FLAG-tagged CLDN16 were incubated in the absence and presence of 200 μM primaquine (*PQ*) for 1 h. *A*, cell lysates were immunoblotted with anti-STX8, FLAG, and β-actin antibodies. *B*, the detergent extracts (*Input*) and cell surface-biotinylated proteins were immunoblotted with anti-FLAG antibody. The cell surface localization of FLAG-tagged CLDN16 was expressed relative to the value in control cells. *C*, cells incubated with primaquine were stained with anti-FLAG (CLDN16) plus ZO-1, STX8, EEA1, or LIMPII antibodies. The *scale bar* represents 5 μm. $n = 3$. **, $p < 0.01$ significantly different from the control.

biotinylation assay, STX8 siRNA decreased the cell surface localization of CLDN16, suggesting that STX8 siRNA inhibits the surface transport or slows down trafficking of CLDN16 from the intracellular compartments to the plasma membrane. The association between cell surface CLDN16 and STX8 was not detected (Fig. 3*F*). We suggest that STX8 can bind to the CLDN16 distributed in cytoplasmic compartments. The cytoplasmic retention of CLDN16 was observed by the treatment with PKI or H-89 (Fig. 6), the mutation at Ser-217 (Fig. 7), a low temperature (Fig. 8), DN-Rab11 (Fig. 10), and primaquine (Fig. 11). These results suggest that the tight junctional localization of CLDN16 may be regulated by its phosphorylation and intracellular trafficking regulators such as STX8 and Rab11.

PKI and H-89 did not affect the expression levels of CLDN16 or STX8 but inhibited the association between CLDN16 and STX8 (Fig. 6). CLDN16 was co-localized with STX8 in the PKI-treated cells (Fig. 6*D*) and in the S217A mutant-expressing cells (Fig. 7*D*), suggesting that both CLDN16 and STX8 were distributed close to each other, whereas STX8 could not transport dephosphorylated CLDN16 from cytoplasmic compartments to the TJ. The physiological role of STX8 on the trafficking of CLDN16 was confirmed by the recycling assay (Fig. 8). Several studies have reported association between STXs and phosphorylated protein. The phosphorylation of Munc18–1 was shown to inhibit the association between Munc18–1 and STX1 and promoted exocytosis (43). A phosphomimetic mutation in SNAP-25 increased the association between SNAP-25 and STX1A (44). Further studies are needed to clarify why dephosphorylated CLDN16 cannot bind to STX8.

A model of calcium depletion showed that TJ protein including CLDN1, CLDN4, occludin, and ZO-1 are internalized by a clathrin-mediated pathway in T84 epithelial cells (45). We also reported that epidermal growth factor promotes endocytosis of CLDN2 mediated by a clathrin-mediated pathway in MDCK cells (20). Clathrin may be a key regulatory factor in endocytosis of TJ protein. In contrast, it has not been reported what regulatory factors are involved in the exocytosis of TJ protein. Our results indicate that STX8 binds to CLDN16 and promotes the exocytosis of CLDN16 from subcellular compartments to the TJ. Prekeris *et al.* (42) reported that STX8 is localized to clathrin-noncoated *trans*-Golgi network and tubulovesicles and suggested that STX8 is involved in trafficking from early endosomes to late endosomes. STX8 may sort and transport CLDN16 via the clathrin-independent trafficking pathway.

STX16 is known to directly interact with cystic fibrosis transmembrane conductance regulator and is involved in regulating the trafficking of cystic fibrosis transmembrane conductance regulator (17). Cystic fibrosis transmembrane conductance regulator is associated with the SNARE domain of STX16. We found that the carboxyl cytoplasmic region of CLDN16 bound to the SNARE domain of STX8 (Fig. 1*D*). The SNARE domain of STX8 may be an important region for binding between STX8 and the carboxyl cytoplasmic region of CLDN16. The cytoplasmic region of CLDN16 contains phosphorylation site (11), and S217A mutant, a dephosphorylated form, was not able to bind to STX8 (Fig. 7). The S217A mutant was co-localized with STX8 in the intracellular compartments. STX8 siRNA increased intracellular distribution of CLDN16 (Fig. 4) without affecting the phosphorylation of CLDN16 (data not shown). We suggest that the association between phosphorylated CLDN16 and STX8 are necessary for the cell surface localization of CLDN16. STX can bind to the clathrin adaptor protein, AP-1, AP-2 (46), AP-3 (47), α-SNAP (38), Munc18 (43), and Vtil-rp1 (38). These proteins are involved in the vesicular fusion and transport. The trafficking of CLDN16 may be regulated by a complex with STX8 and other adaptor proteins.

Taken together, the results of the present study demonstrated that STX8 directly bound to CLDN16 and was involved in the trafficking pathway of CLDN16 in renal tubular epithelial cells. This pathway was found sensitive to temperature, recycling inhibitor primaquine, and Rab11. Most of mutations in the *CLDN16* gene of FHHNC patients and dephosphorylation of CLDN16 induce abnormal cytoplasmic localization. The physiological reabsorption of Mg^{2+} in the TAL of Henle's loop may be dynamically associated with the STX8-regulated expression of CLDN16 in the TJ.

REFERENCES

1. Powell, D. W. (1981) Barrier function of epithelia. *Am. J. Physiol.* **241,** G275–G288
2. Anderson, J. M., Van Itallie, C. M., and Fanning, A. S. (2004) Setting up a selective barrier at the apical junction complex. *Curr. Opin. Cell Biol.* **16,** 140–145
3. Furuse, M., Hirase, T., Itoh, M., Nagafuchi, A., Yonemura, S., and Tsukita, S. (1993) Occludin: a novel integral membrane protein localizing at tight junctions. *J. Cell Biol.* **123,** 1777–1788
4. Furuse, M., Fujita, K., Hiiragi, T., Fujimoto, K., and Tsukita, S. (1998) Claudin-1 and -2: novel integral membrane proteins localizing at tight junctions with no sequence similarity to occludin. *J. Cell Biol.* **141,** 1539–1550
5. Morita, K., Furuse, M., Fujimoto, K., and Tsukita, S. (1999) Claudin multigene family encoding four-transmembrane domain protein components of tight junction strands. *Proc. Natl. Acad. Sci. U.S.A.* **96,** 511–516
6. Tsukita, S., Furuse, M., and Itoh, M. (2001) Multifunctional strands in tight junctions. *Nat. Rev. Mol. Cell Biol.* **2,** 285–293
7. Quamme, G. A., and de Rouffignac, C. (2000) Epithelial magnesium transport and regulation by the kidney. *Front. Biosci.* **5,** D694–D711
8. Simon, D. B., Lu, Y., Choate, K. A., Velazquez, H., Al-Sabban, E., Praga, M., Casari, G., Bettinelli, A., Colussi, G., Rodriguez-Soriano, J., McCredie, D., Milford, D., Sanjad, S., and Lifton, R. P. (1999) Paracellin-1, a renal tight junction protein required for paracellular Mg^{2+} resorption. *Science* **285,** 103–106
9. Konrad, M., Schaller, A., Seelow, D., Pandey, A. V., Waldegger, S., Lesslauer, A., Vitzthum, H., Suzuki, Y., Luk, J. M., Becker, C., Schlingmann, K. P., Schmid, M., Rodriguez-Soriano, J., Ariceta, G., Cano, F., Enriquez, R., Juppner, H., Bakkaloglu, S. A., Hediger, M. A., Gallati, S., Neuhauss, S. C., Nurnberg, P., and Weber, S. (2006) Mutations in the tight-junction gene claudin 19 (CLDN19) are associated with renal magnesium wasting, renal failure, and severe ocular involvement. *Am. J. Hum. Genet.* **79,** 949–957
10. Angelow, S., El-Husseini, R., Kanzawa, S. A., and Yu, A. S. (2007) Renal localization and function of the tight junction protein, claudin-19. *Am. J. Physiol. Renal Physiol.* **293,** F166–F177
11. Ikari, A., Matsumoto, S., Harada, H., Takagi, K., Hayashi, H., Suzuki, Y., Degawa, M., and Miwa, M. (2006) Phosphorylation of paracellin-1 at Ser-217 by protein kinase A is essential for localization in tight junctions. *J. Cell Sci.* **119,** 1781–1789
12. Bock, J. B., Matern, H. T., Peden, A. A., and Scheller, R. H. (2001) A genomic perspective on membrane compartment organization. *Nature* **409,** 839–841
13. McBride, H. M., Rybin, V., Murphy, C., Giner, A., Teasdale, R., and Zerial, M. (1999) Oligomeric complexes link Rab5 effectors with NSF and drive membrane fusion via interactions between EEA1 and syntaxin 13. *Cell* **98,**

377–386
14. Parlati, F., Varlamov, O., Paz, K., McNew, J. A., Hurtado, D., Söllner, T. H., and Rothman, J. E. (2002) Distinct SNARE complexes mediating membrane fusion in Golgi transport based on combinatorial specificity. *Proc. Natl. Acad. Sci. U.S.A.* **99,** 5424–5429
15. Saxena, S., Quick, M. W., Tousson, A., Oh, Y., and Warnock, D. G. (1999) Interaction of syntaxins with the amiloride-sensitive epithelial sodium channel. *J. Biol. Chem.* **274,** 20812–20817
16. Leung, Y. M., Kang, Y., Gao, X., Xia, F., Xie, H., Sheu, L., Tsuk, S., Lotan, I., Tsushima, R. G., and Gaisano, H. Y. (2003) Syntaxin 1A binds to the cytoplasmic C terminus of Kv2.1 to regulate channel gating and trafficking. *J. Biol. Chem.* **278,** 17532–17538
17. Gee, H. Y., Tang, B. L., Kim, K. H., and Lee, M. G. (2010) Syntaxin 16 binds to cystic fibrosis transmembrane conductance regulator and regulates its membrane trafficking in epithelial cells. *J. Biol. Chem.* **285,** 35519–35527
18. Ikari, A., Ito, M., Okude, C., Sawada, H., Harada, H., Degawa, M., Sakai, H., Takahashi, T., Sugatani, J., and Miwa, M. (2008) Claudin-16 is directly phosphorylated by protein kinase A independently of a vasodilator-stimulated phosphoprotein-mediated pathway. *J. Cell. Physiol.* **214,** 221–229
19. Ikari, A., Matsumoto, S., Harada, H., Takagi, K., Degawa, M., Takahashi, T., Sugatani, J., and Miwa, M. (2006) Dysfunction of paracellin-1 by dephosphorylation in Dahl salt-sensitive hypertensive rats. *J. Physiol. Sci.* **56,** 379–383
20. Ikari, A., Takiguchi, A., Atomi, K., and Sugatani, J. (2011) Epidermal growth factor increases clathrin-dependent endocytosis and degradation of claudin-2 protein in MDCK II cells. *J. Cell. Physiol.* **226,** 2448–2456
21. Ikari, A., Nakajima, K., Kawano, K., and Suketa, Y. (2001) Polyvalent cation-sensing mechanism increased Na^+-independent Mg^{2+} transport in renal epithelial cells. *Biochem. Biophys. Res. Commun.* **287,** 671–674
22. Ikari, A., Hirai, N., Shiroma, M., Harada, H., Sakai, H., Hayashi, H., Suzuki, Y., Degawa, M., and Takagi, K. (2004) Association of paracellin-1 with ZO-1 augments the reabsorption of divalent cations in renal epithelial cells. *J. Biol. Chem.* **279,** 54826–54832
23. Ikari, A., Atomi, K., Yamazaki, Y., Sakai, H., Hayashi, H., Yamaguchi, M., and Sugatani, J. (2013) Hyperosmolarity-induced up-regulation of claudin-4 mediated by NADPH oxidase-dependent H_2O_2 production and Sp1/c-Jun cooperation. *Biochim. Biophys. Acta* **1833,** 2617–2627
24. Lanaspa, M. A., Andres-Hernando, A., Rivard, C. J., Dai, Y., and Berl, T. (2008) Hypertonic stress increases claudin-4 expression and tight junction integrity in association with MUPP1 in IMCD3 cells. *Proc. Natl. Acad. Sci. U.S.A.* **105,** 15797–15802
25. Poliak, S., Matlis, S., Ullmer, C., Scherer, S. S., and Peles, E. (2002) Distinct claudins and associated PDZ proteins form different autotypic tight junctions in myelinating Schwann cells. *J. Cell Biol.* **159,** 361–372
26. Murata, M., Kojima, T., Yamamoto, T., Go, M., Takano, K., Chiba, H., Tokino, T., and Sawada, N. (2005) Tight junction protein MAGI-1 is up-regulated by transfection with connexin 32 in an immortalized mouse hepatic cell line: cDNA microarray analysis. *Cell Tissue Res.* **319,** 341–347
27. Hou, J., Shan, Q., Wang, T., Gomes, A. S., Yan, Q., Paul, D. L., Bleich, M., and Goodenough, D. A. (2007) Transgenic RNAi depletion of claudin-16 and the renal handling of magnesium. *J. Biol. Chem.* **282,** 17114–17122
28. Ohta, H., Adachi, H., Takiguchi, M., and Inaba, M. (2006) Restricted localization of claudin-16 at the tight junction in the thick ascending limb of Henle's loop together with claudins 3, 4, and 10 in bovine nephrons. *J. Vet. Med. Sci.* **68,** 453–463
29. Müller, D., Kausalya, P. J., Claverie-Martin, F., Meij, I. C., Eggert, P., Garcia-Nieto, V., and Hunziker, W. (2003) A novel claudin 16 mutation associated with childhood hypercalciuria abolishes binding to ZO-1 and results in lysosomal mistargeting. *Am. J. Hum. Genet.* **73,** 1293–1301
30. Dukes, J. D., Whitley, P., and Chalmers, A. D. (2012) The PIKfyve inhibitor YM201636 blocks the continuous recycling of the tight junction proteins claudin-1 and claudin-2 in MDCK cells. *PLoS One* **7,** e28659
31. Angelow, S., and Yu, A. S. (2009) Structure-function studies of claudin extracellular domains by cysteine-scanning mutagenesis. *J. Biol. Chem.* **284,** 29205–29217
32. Nguyen, N., Kozer-Gorevich, N., Gliddon, B. L., Smolka, A. J., Clayton, A. H., Gleeson, P. A., and van Driel, I. R. (2013) Independent trafficking of the KCNQ1 K^+ channel and H^+-K^+-ATPase in gastric parietal cells from mice. *Am. J. Physiol. Gastrointest. Liver Physiol.* **304,** G157–G166
33. Butterworth, M. B., Edinger, R. S., Silvis, M. R., Gallo, L. I., Liang, X., Apodaca, G., Frizzell, R. A., Fizzell, R. A., and Johnson, J. P. (2012) Rab11b regulates the trafficking and recycling of the epithelial sodium channel (ENaC). *Am. J. Physiol. Renal Physiol.* **302,** F581–F590
34. Cayouette, S., Bousquet, S. M., Francoeur, N., Dupré, E., Monet, M., Gagnon, H., Guedri, Y. B., Lavoie, C., and Boulay, G. (2010) Involvement of Rab9 and Rab11 in the intracellular trafficking of TRPC6. *Biochim. Biophys. Acta* **1803,** 805–812
35. Günzel, D., Haisch, L., Pfaffenbach, S., Krug, S. M., Milatz, S., Amasheh, S., Hunziker, W., and Müller, D. (2009) Claudin function in the thick ascending limb of Henle's loop. *Ann. N.Y. Acad. Sci.* **1165,** 152–162
36. Hou, J., Paul, D. L., and Goodenough, D. A. (2005) Paracellin-1 and the modulation of ion selectivity of tight junctions. *J. Cell Sci.* **118,** 5109–5118
37. Kausalya, P. J., Amasheh, S., Günzel, D., Wurps, H., Müller, D., Fromm, M., and Hunziker, W. (2006) Disease-associated mutations affect intracellular traffic and paracellular Mg^{2+} transport function of Claudin-16. *J. Clin. Invest.* **116,** 878–891
38. Subramaniam, V. N., Loh, E., Horstmann, H., Habermann, A., Xu, Y., Coe, J., Griffiths, G., and Hong, W. (2000) Preferential association of syntaxin 8 with the early endosome. *J. Cell Sci.* **113,** 997–1008
39. Whelton, P. K., and Klag, M. J. (1989) Magnesium and blood pressure: review of the epidemiologic and clinical trial experience. *Am. J. Cardiol.* **63,** 26G–30G
40. Touyz, R. M., and Milne, F. J. (1999) Magnesium supplementation attenuates, but does not prevent, development of hypertension in spontaneously hypertensive rats. *Am. J. Hypertens.* **12,** 757–765
41. Ikari, A., Okude, C., Sawada, H., Sasaki, Y., Yamazaki, Y., Sugatani, J., Degawa, M., and Miwa, M. (2008) Activation of a polyvalent cation-sensing receptor decreases magnesium transport via claudin-16. *Biochim. Biophys. Acta* **1778,** 283–290
42. Prekeris, R., Yang, B., Oorschot, V., Klumperman, J., and Scheller, R. H. (1999) Differential roles of syntaxin 7 and syntaxin 8 in endosomal trafficking. *Mol. Biol. Cell* **10,** 3891–3908
43. Borner, G. H., Rana, A. A., Forster, R., Harbour, M., Smith, J. C., and Robinson, M. S. (2007) CVAK104 is a novel regulator of clathrin-mediated SNARE sorting. *Traffic* **8,** 893–903
44. Yang, Y., Craig, T. J., Chen, X., Ciufo, L. F., Takahashi, M., Morgan, A., and Gillis, K. D. (2007) Phosphomimetic mutation of Ser-187 of SNAP-25 increases both syntaxin binding and highly Ca^{2+}-sensitive exocytosis. *J. Gen. Physiol.* **129,** 233–244
45. Ivanov, A. I., Nusrat, A., and Parkos, C. A. (2004) Endocytosis of epithelial apical junctional proteins by a clathrin-mediated pathway into a unique storage compartment. *Mol. Biol. Cell* **15,** 176–188
46. Heilker, R., Manning-Krieg, U., Zuber, J. F., and Spiess, M. (1996) In vitro binding of clathrin adaptors to sorting signals correlates with endocytosis and basolateral sorting. *EMBO J.* **15,** 2893–2899
47. Darsow, T., Burd, C. G., and Emr, S. D. (1998) Acidic di-leucine motif essential for AP-3-dependent sorting and restriction of the functional specificity of the Vam3p vacuolar t-SNARE. *J. Cell Biol.* **142,** 913–922